JCTC Journal of Chemical Theory and Computation

ARTICLE

pubs.acs.org/JCTC

Multireference Double Electron Attached Coupled Cluster Method with Full Inclusion of the Connected Triple Excitations: MR-DA-CCSDT

Monika Musiał,*[,†] Stanisław A. Kucharski,[†] and Rodney J. Bartlett[‡]

[†]Institute of Chemistry, University of Silesia, Szkolna 9, 40-006 Katowice, Poland

[‡]Quantum Theory Project, Departments of Chemistry and Physics, University of Florida, Gainesville, Florida 32611, United States

ABSTRACT: The multireference (MR) double electron attached (DA) coupled cluster (CC) method with full inclusion of the connected triple excitations has been applied to study various kinds of MR situations. The MR-DA-CCSDT (S, Singles; D, Doubles; T, Triples) equations have been derived and implemented in an efficient way with n^6 scaling for the target multireference states. They can be used for producing potential energy curves (PECs) for some classes of molecules, e.g., when double molecular cations separate into two closed shell fragments, illustrated with the example of the Na_2 molecule. Correct PECs have also been obtained on dissociation of the N−N and C−C bonds in N_2H_4 and C_2H_6 molecules, respectively. Another application is the behavior of the molecular energy when we change dihedral angle in the ethylene molecule: with the MR-DA-CC, we see immediate improvement of the results with smooth, cusp free, behavior around the 90° region.

INTRODUCTION

The equation-of-motion coupled cluster (EOM-CC)[1−12] method has been shown to be a very useful tool in the study of excited, ionized, and electron attached states with many applications.[13−17] However, there is no systematic treatment of the double ionized or doubly electron attached states. The EOM-CC formalism developed for the double ionization (DI) and double electron attachment (DA) issues is no more complicated than those derived for the ionization potential (IP) and electron attachment (EA) or excitation energy (EE) problems and can even have lower computational scaling. But in order to achieve tractable equations, we need to take advantage of the various factorization procedures which formally complicate the equations but significantly reduce the computational effort.

Another reason why the DA and DI problems have attracted less attention is that their experimental verification is more difficult. However, both DI and DA approaches can be successfully used—as we are going to show in this work—to evaluate other molecular properties than direct DA values. The terminology multireference (MR) DA-CC pertains to approximations that can be made in R that are similar to those in MR configuration interaction (CI) and found to be quite important but lie outside the standard approximations anticipated in EOM-CC. The first is to have different levels of excitation operators in R and in T,[18] and this, in particular, provides a MR-DA-CCSD (S, Singles; D, Doubles) solution that is virtually identical to MR-DA-CCSDT (T, Triples), at $\sim n^2$ less cost.

In previous work, we developed the EOM-CC scheme for DI calculations (DI-EOM-CC=MR-DI-CC)[19] (see also similar theoretical works[20,21]). The double ionization potential quantities[20−27] are in many cases experimentally available, for example, via Auger spectroscopy, double charge transfer spectroscopy (DCT), and/or treshold photoelectron coincidence spectroscopy (TPEsCO). Much less attention has been paid to the DA topic since the latter represents a more complex problem from the experimental viewpoint, and also the theoretical apparatus used to extract the required quantities from the experimental data is much more involved.[22,28−30] However, DA calculations, including some earlier work based on the similarity transformed EOM (STEOM)[22,28−30] limited to CCSD,[22,28] are suited to generating potential surfaces or for calculating excitation energies for some systems with pronounced multireference character. The determination of excitation energies via the double electron attachment scheme also corresponds to obtaining wave functions as proper spin-eigenfunctions provided the doubly positive ion is closed shell. This feature is extremely important for open-shell systems, as even normal single-reference (SR), SR-CC theory is notoriously hard to spin-adapt for such cases,[31] not to mention CC's MR generalizations. Satisfying this spin property automatically is a major computational and conceptual simplification.

In this paper, we present the explict equations to calculate DA-EOM-CC and MR-DA-CC. Unlike other MR-CC methods, the method lends itself to "black-box" application. We illustrate the methods for several examples of bond-breaking into radical products, while exclusively using restricted Hartree−Fock (RHF) references and proper spin-eigenfunctions. We also address the question of excitation energies for open-shell atoms and the notorious example of twisted ethylene. Because of the favorable treatment of essential effects of triple excitations, MR-DA-CCSD≃MR-DA-CCSDT provides a very economical description of traditional multireference problems with scaling no worse than CCSD itself.

THEORY

In the coupled cluster theory, the wave function $|\Psi_o\rangle$ is defined via the exponential Ansatz

$$|\Psi_o\rangle = e^T|\Phi_o\rangle \quad (1)$$

Received: March 22, 2011
Published: September 14, 2011

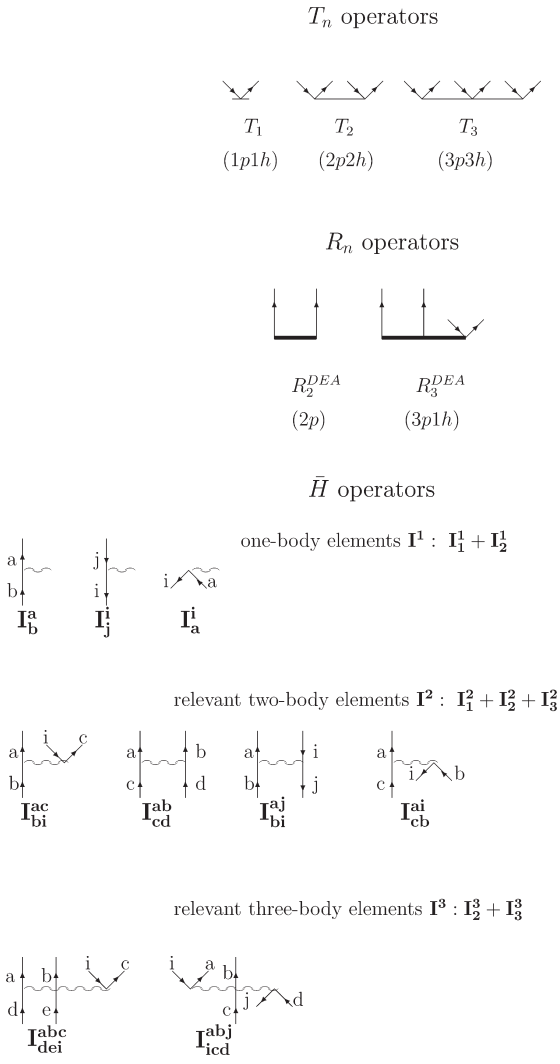

Figure 1. Diagrammatic form of the T, R, and $\overline{H}$ (i.e., I_k^n elements: n-body with k annihilation lines) operators used in the MR-DA-CCSDT method. Types of lines used in the definition of the T and R operators: p, particle; h, hole.

where T is a cluster operator and $|\Phi_o\rangle$ is the reference determinant. Within the CCSDT model, the cluster operator is limited to triple excitations $T = T_1 + T_2 + T_3$ with the usual definition: $T_k = (k!)^{-2} \sum_{ab\ldots}\sum_{ij\ldots} t_{ij\ldots}^{ab\ldots}\{a^+b^+\ldots ji\}$, where the indices a, b, ...(i, j, ...) refer to virtual (occupied) one-particle levels. The Schrödinger equation is written in the form $H_N|\Psi_o\rangle = \Delta E_o|\Psi_o\rangle$, where $H_N = H - \langle\Phi_o|H|\Phi_o\rangle$ and ΔE_o is the correlation energy. The cluster amplitudes, $t_{ij\ldots}^{ab\ldots}$, are obtained by solving the CC equations, $\langle\Phi_{ij\ldots}^{ab\ldots}|(H_N\, e^T)_c|\Phi_o\rangle = 0$.

Within the EOM formalism, the k-state wave function ($|\Psi_k\rangle$) is obtained by the action of an $R(k)$ operator on the ground state (GS) wave function ($|\Psi_o\rangle$):

$$|\Psi_k\rangle = R(k)|\Psi_o\rangle \quad k = 1, 2, \ldots \tag{2}$$

The $R(k)$ is linear (CI-like), and its choice depends on the particular process. For the double electron attachment, it can be expressed as (see Figure 1 for the diagrammatic form of it):

$$R(k) = R_2(k) + R_3(k) \tag{3}$$

where we limit the cluster expansion to the double and triple components (the R_1 part cannot be defined within the DA formalism). The $R(k)$ operator can be expressed through the elementary creation−annihilation operators as

$$R(k) = \frac{1}{2}\sum_{ab} r^{ab}(k)\{a^+b^+\} + \frac{1}{6}\sum_{abc}\sum_{i} r_i^{abc}(k)\{a^+b^+c^+i\} \tag{4}$$

Thus, for the double electron attachment problem, we create electrons in levels a and b ($R_2(k)$), or in addition, we add single excitation from i to c ($R_3(k)$). These single excitations are sometimes called S_1 in the following. The effect of $\{a^+b^+\}$ working on an $n-2$ electron vacuum, which is a kind of "core" vacuum, generates four determinants composed of two "valence" orbitals that can become quasi-degenerate, thereby naturally introducing the four determinant MR description of the problem. Then, S_1 accounts for single excitations among these four determinants, analogous to adding singles to a MR-CI. Such terms are extremely important. In principle, further excitations could be made from the "CI" side of the Ansatz. The choice of orbitals to use in the $n-2$ electron vacuum is arbitrary, and many different choices were considered in our prior paper.[19] But, the obvious choice for the DA case is HF core orbitals, since these do not have most of the pathologies that can be encountered in the DI problem.

The Schrödinger equation for the double electron-attached states (k = 1, 2, ...) can be written as

$$H_N R(k)|\Psi_o\rangle = \Delta E_k R(k)|\Psi_o\rangle \tag{5}$$

Taking advantage of the definition of the CC wave function, eq 1, after simple algebra we arrive at the final EOM equation in the form

$$\bar{H}_N R(k)|\Phi_o\rangle = \omega_k R(k)|\Phi_o\rangle \tag{6}$$

where $\overline{H}_N$ is the similarity transformed Hamiltonian defined as

$$\bar{H}_N = e^{-T} H\, e^T - \langle\Phi_o|e^{-T} H\, e^T|\Phi_o\rangle \tag{7}$$

and the $\omega_k = \Delta E_k - \Delta E_o$ is the energy change connected with the double electron-attachment process.

In the matrix form, eq 6 can be written as

$$\bar{\mathbf{H}}_\mathbf{N}\mathbf{R}(\mathbf{k}) = \omega_k \mathbf{R}(\mathbf{k})$$

A diagonalization of the matrix $\overline{\mathbf{H}}_\mathbf{N}$ in the subspace of double-electron attached configurations provides required energies and eigenvectors.

As is known,[12] the single electron-attachment R operator (presented as linear in the EOM formalism) can be obtained also in the linear form via exponential expansion introduced in the Fock space CC (FS-CC) theory,[32−39] since all products of $S^{(1,0)}$ in $\exp(S^{(1,0)})$ vanish, leaving just $S^{(1,0)} = R$. This makes EA-EOM-CC entirely linked, connected, extensive, and intensive for principal EAs. For EE-EOM-CC, all excited states are intensive, but since $R(k)$ does not correspond to $\exp(S^{(1,1)})$,[32,34,35,40] the equations are not composed solely of linked diagrams. The same refers to the double attached states (two valence sector in FS formalism: (2,0)). But if deemed important, as shown in ref 41, there is a possibility to eliminate this drawback of the EE-EOM-CC theory via EOM-CCx (size-extensive EOM-CC) strategy based on the Canonical Bloch Equation of FS-CC,[42] but at the cost of introducing a choice of "active orbitals". We do not want to do that here, since the transparency of the MR-DA-CC theory to active orbitals is one of its primary advantages.

It is well-known that $\overline{\mathbf{H}}_\mathbf{N}$ is a non-Hermitian matrix, so there is a left-hand eigenvector, $\mathbf{L}(\mathbf{k})\overline{\mathbf{H}}_\mathbf{N} = \omega_\mathbf{k}\mathbf{L}(\mathbf{k})$. Both $\mathbf{L}(\mathbf{k})$ and $\mathbf{R}(\mathbf{k})$ eigenvectors have the same ω_k eigenvalue, and both are needed to obtain ordinary and transition density matrices.

Since the EOM scheme can be viewed in a CI-like way, it can be reduced to the diagonalization of a matrix within the appropriate configurational subspace. At the CCSD level for the DA case, we diagonalize a smaller matrix than for the EA problem:[12]

$$\bar{\mathbf{H}} = [\langle \mathbf{D}|\bar{\mathbf{H}}|\mathbf{D}\rangle]$$

where $D \equiv \Phi^{ab}$ represents the Slater determinants corresponding to the double electron attached configurations. At the "triples" level, we would have an additional configuration of the type T ($\equiv \Phi_i^{abc}$, i.e., double attachment is accompanied by single excitation, S_1, contributing to R):

$$\bar{\mathbf{H}} = \begin{bmatrix} \langle \mathbf{D}|\bar{\mathbf{H}}|\mathbf{D}\rangle & \langle \mathbf{D}|\bar{\mathbf{H}}|\mathbf{T}\rangle \\ \langle \mathbf{T}|\bar{\mathbf{H}}|\mathbf{D}\rangle & \langle \mathbf{T}|\bar{\mathbf{H}}|\mathbf{T}\rangle \end{bmatrix}$$

When we use a CCSD reference state but add R_3 terms into R, we get most of the benefits of triples without ever having to build the CCSDT solution, which would add an $\sim n_{\mathrm{occ}}^3 n_{\mathrm{vir}}^5$ step in its evaluation. That mixture of terms leads to the MR-DA-CCSD viewpoint.

MR-DA-CC Working Equations. In this section, we present explicit working equations for the MR-DA-CC method. This requires solution of the standard CC equations to provide the T_n amplitudes and then the construction of the $\overline{H}$ operator, according to eq 7. To obtain the eigenvalues and eigenvectors of the $\overline{H}$ operator, we employ a direct diagonalization scheme for non-Hermitian matrices[43] analogous to the standard Davidson method.[44] When the right-hand solutions are sought, the Davidson scheme requires the product of the MR-DA-CC matrix right multiplied by the amplitude vector R, i.e., $\overline{H}R$. When R and T correspond to the same level of excitation, MR-DA-CC = DA-EOM-CC

We consider two models for the DA problem based on the CCSD and CCSDT solutions. The former requires determination of the R_2 (i.e., 2p; p, particle) amplitudes only and the latter, both R_2 (i.e., 2p) and R_3 (i.e., 3$p1h$; h, hole).

DA-EOM-CC is exactly MR-DA-CCSD without S_1 and is quite simple. It is presented in Figure 2a in a diagrammatic form and in Table 1 (in the CCSD section) in an algebraic form. At the CCSDT level, the DA equations are much more complicated, see Figure 2b or the lower part of Table 1. Note that to each term in Table 1 the proper permutation of the external indices should be applied, as indicated by the symbol $P(.../...)$ (see the explanation given in the footnote to Table 1). It should be explained also that in Tables 1 and 2 we adopt the tensor notation, which implies summation over repeated indices.

The form of $\overline{H}$ required for the construction and solution of the MR-DA-CCSDT equations in their standard form involves up to three-body elements. Emphasizing the many-body structure of $\overline{H}$, we may decompose it into individual contributions as follows:

$$\bar{H} = I^1 + I^2 + I^3 \tag{8}$$

We may rewrite the particular element, I^n, as the sum over components I_k^n, where k indicates the number of annihilation lines (see Figure 1):

$$\begin{aligned} I^1 &= I_1^1 + I_2^1 \\ I^2 &= I_1^2 + I_2^2 + I_3^2 \\ I^3 &= I_2^3 + I_3^3 \end{aligned} \tag{9}$$

We skipped the $\overline{H}$ components with 0 annihilation lines since they cannot be contracted with the R operators. Similarly, in the last equation, the I_1^3 term is omitted since it does not enter the MR-DA-CCSDT model. The same refers to the I_4^2 element of $\overline{H}$

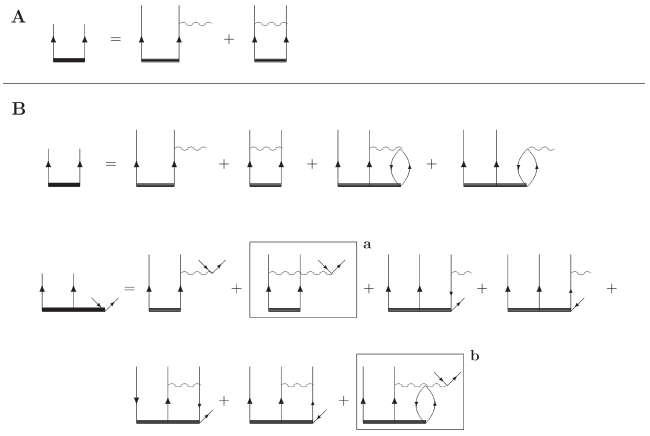

Figure 2. Diagrammatic form of the MR-DA-CC equations (**A**, MR-DA-CCSD no S_1 variant; **B**, MR-DA-CCSDT variant) in antisymmetrized formalism for the standard version.

Table 1. MR-DA-CCSD no S_1 and MR-DA-CCSDT Equations in Goldstone Formalism for Standard and Factorized Version

expression[a]
MR-DA-CCSD no S_1
$(\overline{H}R)^{ab} = P(a/b)[r^{ae}I_e^b + 1/2r^{ef}I_{ef}^{ab}]$
MR-DA-CCSDT
$(\overline{H}R)^{ab} = P(a/b)[r^{ae}I_e^b + 1/2r^{ef}I_{ef}^{ab} + 2r_m^{aef}I_{ef}^{bm} - r_m^{aef}I_{ef}^{mb} - r_m^{efb}I_{ef}^{am} + r_m^{abe}I_e^m - r_m^{aeb}I_e^m]$
$(\overline{H}R)_i^{abc} = P(a/b)[r^{ae}I_{ei}^{bc} + 1/2r_i^{abe}I_e^c + 1/2r_m^{abc}I_i^m + r_i^{ebc}I_e^a + 1/2r_i^{efc}I_{ef}^{ab} + r_i^{aef}I_{ef}^{bc} - r_m^{aec}I_{ei}^{bm} - 1/2r_m^{abe}I_{ie}^{mc} + r_m^{abe}I_{ei}^{mc} - r_m^{aeb}I_{ei}^{mc}] + F_i^{abc}$
$F_i^{abc\ b} = P(a/b)[1/2r^{ef}I_{efi}^{abc} + 2r_m^{aef}I_{efi}^{bmc} - r_m^{aef}I_{efi}^{mbc} - r_m^{efb}I_{efi}^{amc}]$
$F_i^{abc\ c} = P(a/b)[1/2t_{mni}^{abc}\chi^{mn} - t_{mi}^{bc}\chi^{am}]$

[a] Summation over repeated indices assumed on the right-hand side. Summation indices belong to the set $\{e,f,m,n\}$. $P(a/b)$ implies the sum of two components differing by permutation of a and b. All elements of $\overline{H}$ ($I_{tu...}^{rs...}$) are defined in refs 11 and 12, whereas the intermediates ($\chi_{t...}^{r...}$) are defined in Table 2. [b] Standard version. [c] Factorized version.

Table 2. Algebraic Expression for the χ Intermediates Used in the MR-DA-CCSDT Model

intermediate	expression[a]
χ^{ij}	$+ r^{ef}v_{ef}^{ij}$
χ^{ai}	$+ r^{ef}I_{ef}^{ai} + 2r_m^{aef}v_{ef}^{im} - r_m^{efa}v_{ef}^{im} - r_m^{aef}v_{ef}^{mi}$

[a] Summation over repeated indices assumed; summation indices belong to the set $\{e,f,m\}$.

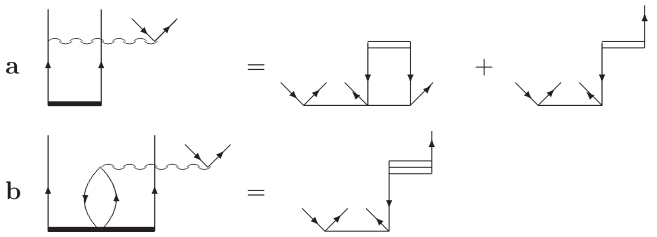

Figure 3. Diagrammatic notation of the factorization of selected contributions to the MR-DA-CC equations.

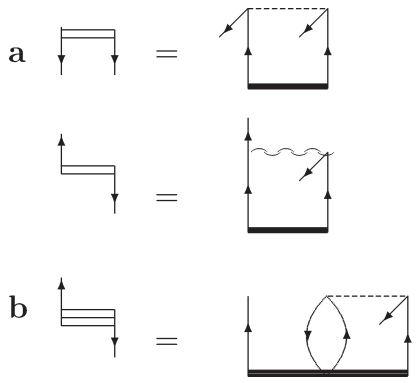

Figure 4. Diagrammatic form of the intermediates used in the MR-DA-CCSDT equations in antisymmetrized formalism.

in the second equation. We apply here our diagrammatic formalism, which is discussed, for example, in refs 13 and 14.

The many-body type of the $\overline{H}$ elements expressed through the $I^{r\ldots}_{t\ldots}$ amplitudes are determined by the number of indices, i.e., I^{r}_{s}, I^{rs}_{tw} and I^{rst}_{uvw}, corresponding to the I^1, I^2, and I^3 operators, respectively. Note that the *r,s,...* symbols indicate general indices being of either hole or particle character.

It is easy to also assign creation−annihilation character to the particular $I^{r\ldots}_{s\ldots}$ amplitude. The index referring to the annihilation (creation) line is represented by the presence of the hole (particle) symbol as a superscript or the particle (hole) symbol as the subscript. To clarify this point, we give the following definition of the I^n_k elements expressed through their regular, antisymmetrized form:

$$
\begin{aligned}
I^1_1 &= \sum_{a,b} I^a_b a^\dagger b + \sum_{i,j} I^i_j i^\dagger j \\
I^1_2 &= \sum_{a,i} I^i_a i^\dagger a \\
I^2_1 &= \sum_{a,b,c,i} I^{ac}_{bi} a^\dagger c^\dagger i b \\
I^2_2 &= \sum_{a,b,c,d} I^{ab}_{cd} a^\dagger b^\dagger d c + \sum_{a,b,i,j} I^{aj}_{bi} a^\dagger j^\dagger i b \\
I^2_3 &= \sum_{a,b,c,i} I^{ai}_{cb} a^\dagger i^\dagger b c \\
I^3_2 &= \sum_{a,b,c,d,e,i} I^{abc}_{dei} a^\dagger b^\dagger c^\dagger i e d \\
I^3_3 &= \sum_{a,b,c,d,i,j} I^{abj}_{icd} a^\dagger b^\dagger j^\dagger d c i
\end{aligned}
\qquad (10)
$$

All contributions to the elements of the $\overline{H}$ operator used in the MR-DA-CC models proposed in this work are defined in refs 11 and 12.

The MR-DA-CC equations assume that we use all required $\overline{H}$ elements regardless of the complexity of a particular term. This means that we employ all appropriate three-body terms. That form of the MR-DA-CCSDT equations is presented diagrammatically in Figure 2b and—in its algebraic form—in the *b* equations in Table 1. Such a formulation of the MR-DA-CC problem, although the most natural one, would result in higher scaling of the computational procedure either in the $\overline{H}$ construction or in the solution of the EOM-CC equations. To avoid this, we apply a factorization scheme which naturally accounts for the difficult terms that involve the three-body $\overline{H}$ elements. These terms are indicated in Figure 2b by the rectangles, and their factorized construction is explained in Figures 3 and 4. Hence, the diagram indicated by the letter *a* in the R_3 equation in Figure 2b is replaced by the contribution given in Figure 3a, where the heavy horizontal line corresponds to the *R* amplitude and the thin one to the *T* amplitude (see also Figure 1 for definition of the operators). Thus, we avoid using any explicit three-body $\overline{H}$ element in the R_3 equation by construction of the intermediate shown in Figure 4a and then by employing it in the diagram on the right-hand side of the equation in Figure 3a. The same procedure is applied to diagram *b* in Figure 2b. By the intermediate, we understand throughout the paper the quantity obtained by the contraction of the integral or $\overline{H}$ element with the *R* operator.

The factorization procedure shown diagrammatically in Figures 3 and 4 is shown algebraically in Table 1, where the contribution denoted by F^{abc}_i represents the terms corresponding to the diagrams indicated by rectangles in Figure 2b. The expression for F^{abc}_i is constructed in a standard, nonfactorized way, engaging only $\overline{H}$ elements and *R* amplitudes, see $F^{abc\,b}_i$, or in a factorized way, see $F^{abc\,c}_i$. The latter requires construction of the intermediates χ defined in Table 2.

The factorization procedure makes the evaluation of the $(\overline{H}R)$ quantities much more efficient. We should remember, however, that the $\overline{H}$ elements are computed only once in the whole process, while the intermediates must be recomputed in each iteration. However, that is a most efficient step.

Approximations. As we can see, the equations for the DA amplitudes are much simpler than those for the EA case.[12] In addition, the DA part scales only as $n^6(n^1_{\mathrm{occ}}n^5_{\mathrm{vir}})$ at the CCSDT level. We also do calculations using the MR-DA-CCSD variant in which the GS is the CCSD one (scaling $n^6(n^2_{\mathrm{occ}}n^4_{\mathrm{vir}})$) instead of CCSDT (scaling $n^8(n^3_{\mathrm{occ}}n^5_{\mathrm{vir}})$), and in the EOM part we take R_2 and R_3 as in the full CCSDT model. For comparison purposes, we also implement DA-EOM-CCSD(=MR-DA-CCSD no S_1 variant). The DA part scales as $n^4(n^4_{\mathrm{vir}})$, as it contains only the R_2 equation (first two diagrams in Figure 2). Finally, we consider an additional variant in which we replace the GS CCSDT[45,46] with an approximate version CCSDT-3,[47] termed, MR-DA-CCSDT-3. This variant relies on employing a rigorous treatment of R_2 and R_3 with the ground state CC scaling as $n^3_{\mathrm{occ}}n^4_{\mathrm{vir}}$. The approximate variant behaves in the same manner as its rigorous counterpart (see the Results section), and it can be applied for larger systems for which the effect of triples is essential. We may use the approximate MR-DA-CCSDT-3=DA-EOM-CCSDT-3 method without significantly lowering the accuracy.

RESULTS

A. Twisted Ethylene. The newly implemented methods are applied for the widely known twisted ethylene case[48]

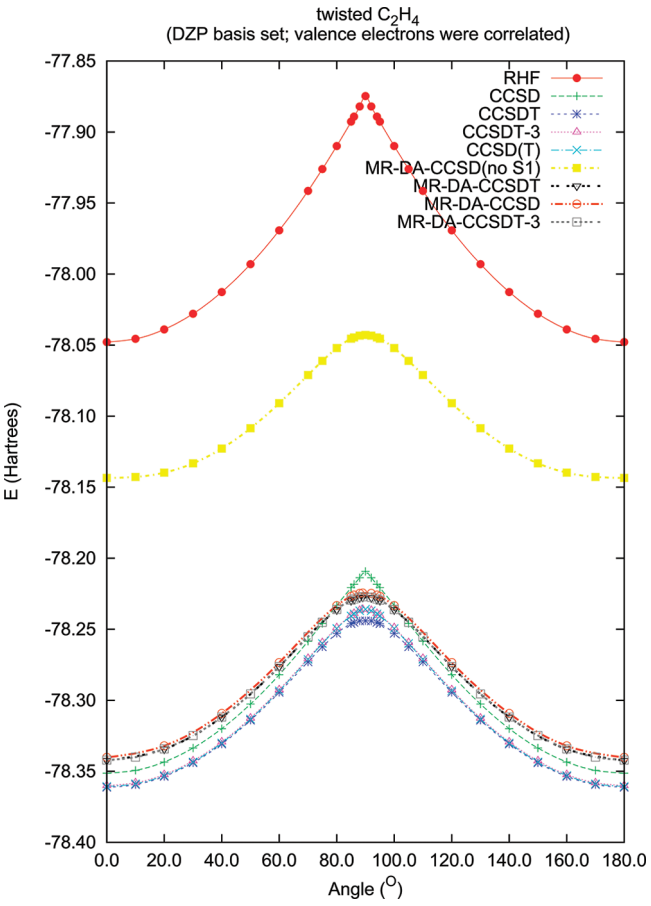

Figure 5. The RHF, CC, and MR-DA-CC torsional curves for the twisted ethylene in DZP basis set and valence electrons correlated (R_{CC} = 1.3390 Å, R_{CH} = 1.0856 Å, $\angle_{HCH}$ = 117.6°).

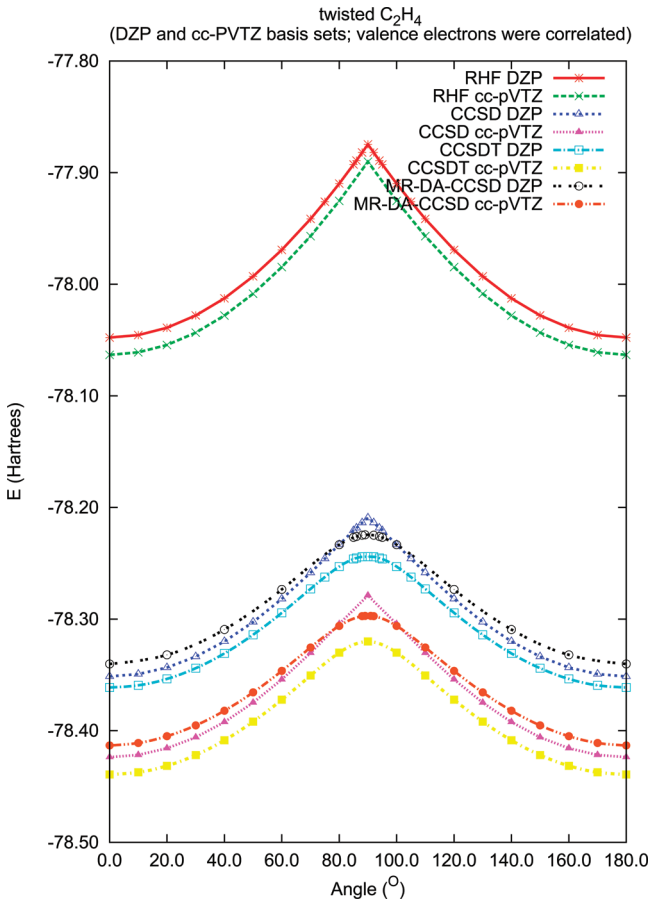

Figure 6. The RHF, CCSD, CCSDT, and MR-DA-CCSD torsional curves for the twisted ethylene in DZP and cc-pVTZ basis sets and valence electrons correlated (R_{CC} = 1.3390 Å, R_{CH} = 1.0856 Å, $\angle_{HCH}$ = 117.6°).

(see Figures 5 and 6), which has a multireference effect. In the calculations, we use DZP[49] and cc-pVTZ[50] basis sets with valence electrons correlated and the experimental geometry R_{CC} = 1.3390 Å, R_{HC} = 1.0856 Å, and $\angle_{HCH}$ = 117.6°. The energy is plotted as a function of the dihedral angle between the two methylene (CH_2) groups. At the very top, we have the SCF curves which show the cusp for 90°. The same is shown by the standard CCSD model, but when using the DA strategy we obtain a smooth curve in the critical region of the potential energy curve (PEC). The same effect is observed for both basis sets employed; the cc-pVTZ curves are slightly shifted toward lower energy, but the two sets are parallel. When adding triples, the DA curves are of the same shape and without the typical cusp retained in CCSD total energy. The DA calculations are performed in such a way that we do ground state CC calculations for the double cation, and the neutral molecule energy is obtained with DA eigenvalues. For the planar conformation, we have no problem with applying any quantum chemical method, but when the dihedral angle is changed to the 90° conformation, then the HOMO−LUMO gap becomes small, and we encounter various divergencies, demonstrating its MR character. To the contrary, when we do calculations for the double-electron attached molecule (alternatively for the double ionized molecule[19]), the problem disappears. Thus, we can use MR-DA-CC methods to obtain an accurate description of some of the traditional multireference situations.

B. Sodium Dimer. The next example of the application of the new method is the PEC for the Na_2 molecule (see Figures 7 and 8). The calculations use the POL1[51] basis set, and the 1s orbitals are kept frozen. In the $n-2$ reference, the Na_2 system is a closed shell one. Doing calculations around the equilibrium using standard methods is straightforward, but when we try to do, for example, the whole potential energy curve, then for larger R we may have problems with obtaining the reference function since Na_2 would dissociate into two open-shell fragments (Na atoms). However, when we do calculations using the DA strategy, we do it for the Na_2^{+2} cation, which dissociates into two closed shell fragments (isoelectronic with neon atom). The essence of this trick relies on the fact that DA calculations for the Na_2^{2+} for large R are much easier to carry to complete separation as spin-eigenstates. In Figure 7, we see that all curves representing the MR-DA methods based on the full R_3 approximation stay close to the CCSDT curve (which is considered here a reference one) irrespective of the CC model used for the GS. Incorrect behavior is observed for the R_2 only model (no R_3; top curve) and also for the noniterative CCSD(T) curve, showing a hump around 6 Å .

In Figure 8, we show the nonparallelity error curve representing the differences between the reference CCSDT values and the MR-DA-CCSD ones. Nearly within the whole range of the internuclear distances, they are very stable and small (ca. 3.6 mH),

dx.doi.org/10.1021/ct200195q |J. Chem. Theory Comput. 2011, 7, 3088–3096

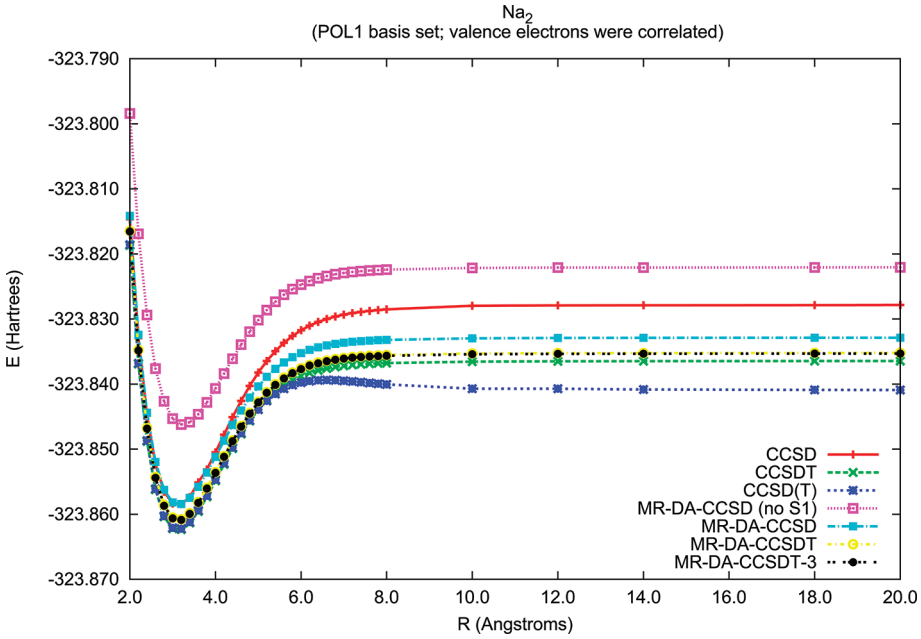

Figure 7. Potential energy curves for the Na_2 molecule with MR-DA-CC and CC methods.

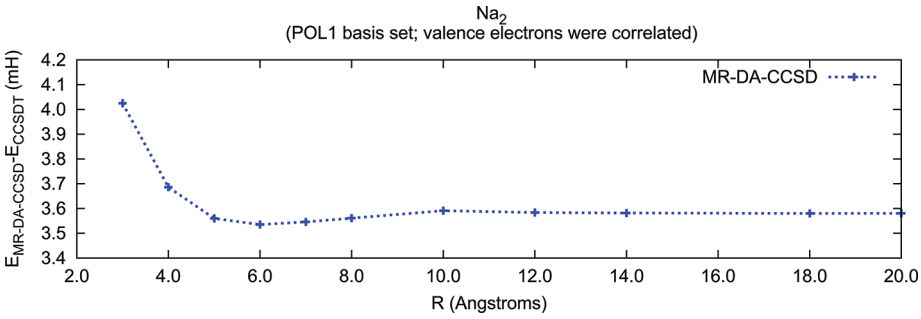

Figure 8. Energy difference from CCSDT for Na_2 ground state MR-DA-CCSD.

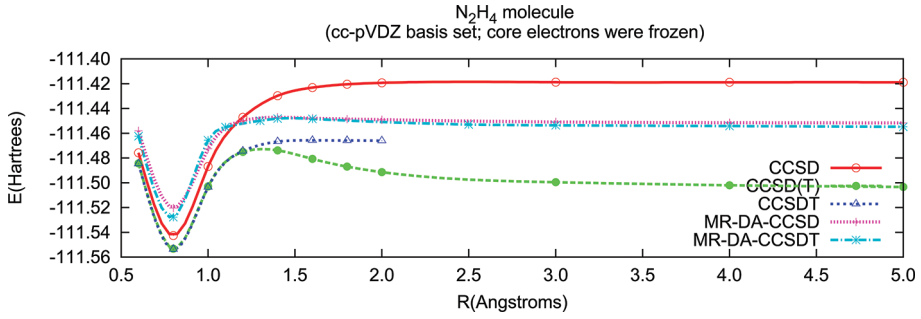

Figure 9. The CC and MR-DA-CC curves for the N_2H_4 molecule in the cc-pVDZ basis set and valence electrons correlated (R_{NH} = 1.016 Å, $\angle_{HNN}$ = 108.85°, $\angle_{HNH}$ = 106°).

going up to 4.0 mH at short R values. As will be presented elsewhere, this underbinding near equilibrium does not happen with the MR-DI-CCSD version. We attribute the differing results to defects of using the double cation orbitals in the MR-DA-CCSD results presented here, but there are also other aspects to consider. In the bond-breaking MR regions of the curves, though, MR-DA-CCSD is excellent and seems to be better than its MR-DI-CCSD counterpart.

In the context of the Na_2 dissociation, we should mention the size-extensivity issue. A characteristic feature of the EOM theory is its size-intensivity, which states that upon separation of two fragments ($AB^* \rightarrow A^* + B$) the energies corresponding to the local excitation (or local double ionization or local double-electron attachment) are size-extensive. When the process in question engages both fragments, e.g., a charge-transfer excitation in EE-EOM-CC, then the equations do not correspond to a

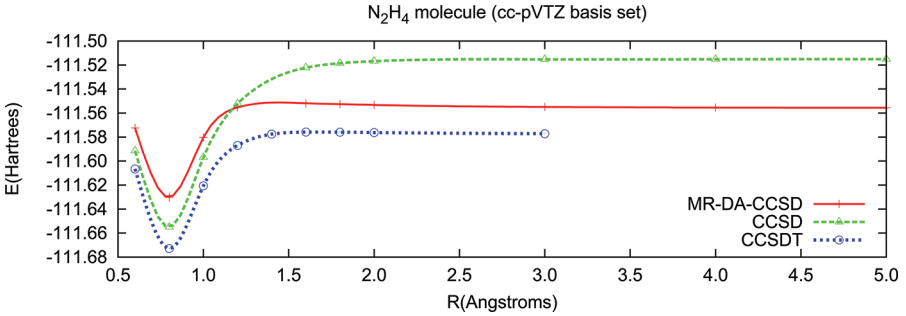

Figure 10. The CCSD and MR-DA-CCSD curves for the N_2H_4 molecule in the cc-pVTZ basis set (frozen orbitals: first two occupied and 11 highest unoccupied ones; R_{NH} = 1.016 Å, $\angle_{HNN}$ = 108.85°, $\angle_{HNH}$ = 106°).

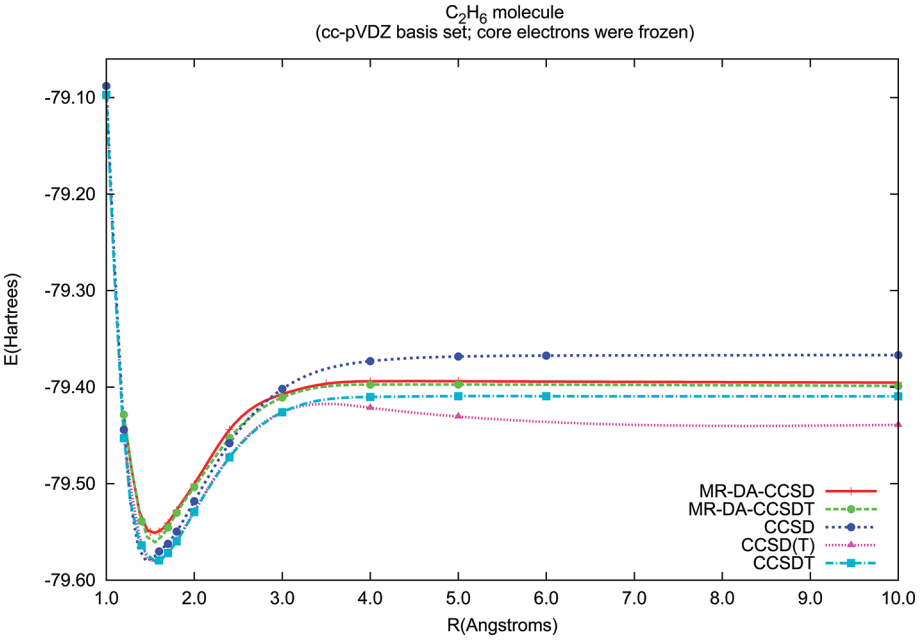

Figure 11. The CC and MR-DA-CC curves for the C_2H_6 molecule in the cc-pVDZ basis set and valence electrons correlated (R_{CH} = 1.091 Å, $\angle_{HCC}$ = 110.91°, $\angle_{HCH}$ = 108°).

fully linked form, and the dissociation of the Na_2 ground state belongs to this category. This feature occurs because the terms involved for both fragments correspond to higher excitations than are included in the level of the calculation like CCSD. So this is not as much a failure of the theory as its truncation to singles and doubles, for example. The question of size-intensive quantities being the difference between two size-extensive ones, or just size-intensive without that condition, is an interesting one.

C. Hydrazine. In Figure 9, we show PECs for the N−N bond of the N_2H_4 molecule with three computational methods of SR character (CCSD, CCSDT, and CCSD(T)) and two MR-DA based on the CCSD and CCSDT reference obtained for the cc-pVDZ[50] basis set. In Figure 10, we plot three potential energy curves obtained for CCSD, CCSDT, and MR-DA-CCSD schemes using a cc-pVTZ basis set.[50] For the CCSDT in both basis sets, the convergence can be reached only for R values no longer than 2−3 Å . For the CCSD scheme, the CC equations converge within the whole range of R values, but the curve is too high. The CCSD(T) shows its typical failure with a hump around 1.2 Å. The MR-DA curves show correct behavior for both basis sets and for two types of GS references. The obvious inadequacy of the MR curves is a too high energy around equilibrium that we believe can be remedied, partly by employing orbitals optimized for the n electron problem instead of the $n - 2$ one used in the current work.

D. Ethane. Similar observations can be made with respect to the dissociation of the C−C bond and resulting PECs for the C_2H_6 molecule, see Figures 11 and 12. We show the same set of PECs as for the N_2H_4 molecule both for the cc-pVDZ (Figure 11) and cc-pVTZ (Figure 12) basis sets. The observations are similar: both MR curves shown in Figure 11 stay close to the CCSDT reference, and the same is true for the MR-DA-CCSD curve shown in Figure 12. In the case of the C_2H_6 system, the single reference CCSDT curve can be obtained for the whole range of R values. Both the SR CCSD curves (Figures 11 and 12) deviate toward higher energies, which visibly worsens the performance of the CCSD model. Though the results for N_2H_4 and C_2H_6 molecules are qualitatively similar at all MR levels, the MR-DA curves based on the CCSD reference are computed with significantly lower computer effort than those based upon CCSDT.

MR-DA results can be seen as an alternative route to evaluate potential energy curves for the ground and excited states. The

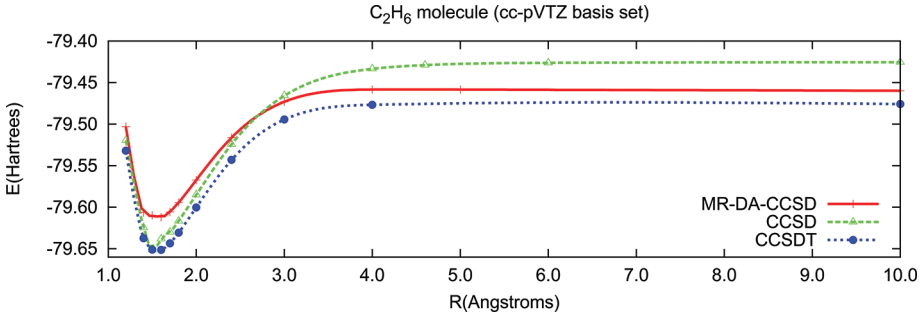

Figure 12. The CCSD and MR-DA-CCSD curves for the C_2H_6 molecule in the cc-pVTZ basis set (frozen orbitals: first two occupied and 41 highest unoccupied ones; R_{CH} = 1.091 Å, $\angle_{HCC}$ = 110.91°, $\angle_{HCH}$ = 108°).

Table 3. Excitation Energies (eV) for the C Atom Using the MR-DA-CC Methods in the POL1 Basis Set

	MR-DA-CC					
	SD (no S_1)	SDT	SD	SDT-3	AEL[a]	exptl[b]
	$T = T_1 + T_2$[c]	$T = T_1 + T_2 + T_3$[d]	$T = T_1 + T_2$[c]	$T = T_1 + T_2 + T_3$[e]		
sym.	$R = R_2$	$R = R_2 + R_3$	$R = R_2 + R_3$	$R = R_2 + R_3$		
$2p^2\ ^3P$	0.0	0.0	0.0	0.0	91.5%	0.0
$2p^2\ ^1D$	1.308	1.480	1.481	1.480	92.7%	1.26
$2p^2\ ^1S$	1.771	2.802	2.805	2.801	94.5%	2.68
$2p3s\ ^3P^0$	5.834	7.318	7.320	7.318	95.4%	7.48
$2p3s\ ^1P^0$	5.963	7.520	7.521	7.520	96.7%	7.68
$2p3p\ ^1P$	7.107	8.503	8.504	8.503	95.9%	8.54
$2p3p\ ^3D$	7.228	8.670	8.671	8.670	96.1%	8.64
$2p3p\ ^3S$	7.411	8.869	8.870	8.869	96.1%	8.77
$2p3p\ ^3P$	7.748	9.026	9.027	9.026	94.9%	8.85
$2p3p\ ^1D$	8.051	9.382	9.384	9.382	96.1%	9.00
MAE[f]	1.175	0.154	0.155	0.154		

[a] Approximate excitation level indicates % of the R_2 (i.e., $2p$) configurations. [b] ref 53. [c] GS: CCSD. [d] GS: CCSDT. [e] GS: CCSDT-3. [f] MAE: mean absolute error.

method clearly provides superior bond-breaking subject to RHF reference functions. The results tend to fall between SR-CCSD and SR-CCSDT, but with none of the expense of the latter and better bond breaking behavior with RHF reference functions in either case.

E. Carbon Excitations. Finally, we apply DA calculations to determine the excitation spectra. Though it is planned to treat a number of transition metal atoms in this way, we first illustrate it for the carbon atom which has two electrons out of a closed shell structure. Adding two electrons to the Be configuration of C^{2+}, we can obtain excited states of carbon (see Table 3) in a very economical way. In the calculations, we use the POL1 basis set with 6 d functions and all electrons correlated. We quote in Table 3 the excitation energies for nine low lying states, relating them to the experimental data. Four different methods are considered: one (CCSD) based on the CCSD solution for the ground state and on the EOM-CCSD equation for the DA part. The other methods engage R_3 in the results. The most important column is the third, where the reference state is the CCSD ($n_{occ}^2 n_{vir}^4$) solution and the target states solutions at the DA level are ($\sim n_{occ}^1 n_{vir}^5$), which means single excitations of the MR space generated by the DA operator, $\{a^+b^+\}$. Its inclusion provides nearly identical results to the full inclusion of triples, a remarkable improvement over the DA-EOM-CCSD(=MR-DA-CCSD no S_1) value equal to 1.175 eV (see second column in Table 3). Clearly, the quality of the ground state wave function is less important than that for the target state. The results also compare well with experimental results. In most cases, the deviation remains between 0.04 and 0.20 eV. It grows, however, for the higher energy states.

In Table 3, we also list the AEL (approximate excitation level) values for the computed states of the C atom. In the last column are the percentages of the R_2 type configurations in the computed double-electron attached states. All of the states obtained are dominated by the configurations created by the R_2 operator.

CONCLUSIONS

A new MR-DA-CC method is introduced and applied with full inclusion of the connected triple excitations. When R and T include the same excitation levels, this is simply DA-EOM-CC, but by mixing them with an eye toward MR excitations in the target state, much better results are obtained, and at substantially less cost than the unmodified DA-EOM-CCSDT. By adopting the proper factorization strategy, all terms involving the evaluation of the three-body elements of the $\overline{H}$ operators are bypassed by a rigorous factorization procedure. The factorization makes it possible to achieve a scaling of the target state that is no worse

than $n_{occ}^{1}n_{vir}^{5}$ after the ground state is obtained. All of the resulting equations are presented diagrammatically and algebraically with a detailed presentation of the factorization scheme.

The program developed, part of ACES II,[52] has been subsequently applied to the calculation of the DA for production of the PEC for some systems when double cation separates into two closed shell fragments. The bottleneck of the calculation occurs in the GS calculations. To address this, we propose some approximations with better scaling that yield comparable results to these for the full or more complete methods.

The MR-DA-CC methods are highly suitable for doing calculations for systems that require a traditional multireference description in a very economical, unbiased, and routine way. The double attachment scheme can be used to calculate excitation spectra of open-shell systems. It can be applied to describe systems that have two electrons out of a closed shell structure (i.e., difficult transition states, biradicals, etc.), and it will be generalized to three, four, and more attached states, TA, QA, etc. The approach potentially offers a very attractive, easily applied MR-CC method for many problems.

AUTHOR INFORMATION

Corresponding Author
*E-mail: musial@ich.us.edu.pl.

ACKNOWLEDGMENT

This work has been supported by the Ministry of Science and Higher Education, Poland, under grant No. N N204 090938, and also by the United States Air Force Office of Scientific Research under STTR AF09-BT40.

REFERENCES

(1) Rowe, D. J. *Rev. Mod. Phys.* **1968**, *40*, 153.
(2) Sekino, H.; Bartlett, R. J. *Int. J. Quantum. Chem. Symp.* **1984**, *18*, 255–265.
(3) Geertsen, J.; Rittby, M.; Bartlett, R. J. *Chem. Phys. Lett.* **1989**, *164*, 57–62.
(4) Stanton, J. F.; Bartlett, R. J. *J. Chem. Phys.* **1993**, *98*, 7029–7039.
(5) Comeau, D. C.; Bartlett, R. J. *Chem. Phys. Lett.* **1993**, *207*, 414–423.
(6) Emrich, K. *Nucl. Phys. A* **1981**, *351*, 379–396.
(7) Kucharski, S .A.; Wloch, M.; Musial, M; Bartlett, R. J *J. Chem. Phys.* **2001**, *115*, 8263–8266.
(8) Kowalski, K; Piecuch, P. *J. Chem. Phys.* **2001**, *115*, 643–651.
(9) Korona, T.; Werner, H. J. *J. Chem. Phys.* **2003**, *118*, 3006–3019.
(10) Hirata, S. *J. Chem. Phys.* **2004**, *121*, 51–59.
(11) Musial, M.; Kucharski, S. A.; Bartlett, R. J. *J. Chem. Phys.* **2003**, *118*, 1128–1136.
(12) Musial, M.; Bartlett, R. J. *J. Chem. Phys.* **2003**, *119*, 1901–1908.
(13) Bartlett, R. J.; Musiał, M. *Rev. Mod. Phys.* **2007**, *79*, 291−352 and references therein.
(14) Shavitt, I.; Bartlett, R. J. *Many-Body Methods in Chemistry and Physics: Many-Body Perturbation Theory and Coupled Cluster Methods*; Cambridge Press: Cambridge, England, 2009.
(15) Krylov, A. I. *Annu. Rev. Phys. Chem.* **2008**, *59*, 433–462.
(16) Musial, M; Kucharski, S. A.; Bartlett, R. J. *Adv. Quantum Chem.* **2004**, *47*, 209–222.
(17) Musiał, M. *Mol. Phys.* **2010**, *108*, 2921–2931.
(18) Hirata, S.; Nooijen, M.; Bartlett, R. J. *Chem. Phys. Lett.* **2000**, *326*, 255–262.
(19) Musial, M; Perera, A.; Bartlett, R. J. *J. Chem. Phys.* **2011**, *134*, 114108−1–10.
(20) Sattelmeyer, K. W.; Schaefer, H. F., III; Stanton, J. F. *Chem. Phys. Lett.* **2003**, *378*, 42–46.
(21) Demel, O.; Shamasundar, K. R.; Kong, L.; Nooijen, M. *J. Phys. Chem. A* **2008**, *112*, 11895–11902.
(22) Nooijen, M.; Bartlett, R. J. *J. Chem. Phys.* **1997**, *107*, 6812–6830.
(23) Musiał, M; Bartlett, R. J. *J. Chem. Phys.* **2011**, *135*, 044121−1–8.
(24) Chaudhuri, R.; Datta, B.; Das, K.; Mukherjee, D. *Int. J. Quantum Chem.* **1996**, *60*, 347–358.
(25) Ida, T.; Ortiz, J. V. *J. Chem. Phys.* **2008**, *129*, 084105−1–11.
(26) Schulte, H. D.; Cederbaum, L. S. *J. Chem. Phys.* **1996**, *105*, 11108–11133.
(27) Van Huis, T. J.; Wesolowski, S. S.; Yamaguchi, Y.; Schaefer, H. F., III. *J. Chem. Phys.* **1999**, *110*, 11856–11864.
(28) Tobita, M.; Perera, S. A.; Musial, M.; Bartlett, R. J.; Nooijen, M.; Lee, J. S. *J. Chem. Phys.* **2003**, *119*, 10713–10723.
(29) Eliav, E.; Kaldor, U.; Ischikawa, Y. *Phys. Rev. A* **1996**, *53*, 3050–3056.
(30) Nayak, M. K.; Chaudhuri, R. K. *Eur. Phys.* **2006**, *37*, 171–176.
(31) Piecuch, P.; Paldus, J. *Int. J. Quantum Chem.* **1989**, *36*, 429–453.
(32) Pal, S.; Rittby, M.; Bartlett, R. J. *Chem. Phys. Lett.* **1989**, *160*, 212–218.
(33) Mukhopadhyay, A.; Moitra, R. K.; Mukherjee, D. *J. Phys. B* **1979**, *12*, 1–18.
(34) Mukherjee, D.; Pal, S. *Adv. Quantum Chem.* **1989**, *20*, 291–373.
(35) Meissner, L.; Bartlett, R. J. *J. Chem. Phys.* **1991**, *94*, 6670–6676.
(36) Kaldor, U. *Theor. Chim. Acta* **1991**, *80*, 427–439.
(37) Stolarczyk, L. Z.; Monkhorst, H. J. *Phys. Rev. A* **1985**, *32*, 725–742.
(38) Meissner, L. *J. Chem. Phys.* **1995**, *103*, 8014–8021.
(39) Musiał, M.; Bartlett, R. J. *J. Chem. Phys.* **2004**, *121*, 1670–1675.
(40) Lindgren, I.; Mukherjee, D. *Phys. Rep* **1987**, *151*, 93–127.
(41) Musiał, M.; Bartlett, R. J. *J. Chem. Phys.* **2011**, *134*, 034106−1–12.
(42) Musiał, M.; Bartlett, R. J. *J. Chem. Phys.* **2008**, *129*, 134105−1–12.
(43) Hirao, K.; Nakatsuji, H. *J. Comput. Phys.* **1982**, *45*, 246–254.
(44) Davidson, E. R. *J. Comput. Phys.* **1975**, *17*, 87–94.
(45) Noga, J.; Bartlett, R. J. *J. Chem. Phys.* **1987**, *86*, 7041–7050.
(46) Noga, J.; Bartlett, R. J. *J. Chem. Phys.* **1988**, *89*, 3401.
(47) Noga, J.; Bartlett, R. J.; Urban, M. *Chem. Phys. Lett.* **1987**, *134*, 126–132.
(48) Casanova, D.; Head-Gordon, M. *J. Chem. Phys.* **2008**, *129*, 064104−1–12.
(49) Dunning, T. K., Jr. *J. Chem. Phys.* **1970**, *53*, 2823.
(50) Dunning, T. K., Jr. *J. Chem. Phys.* **1989**, *90*, 1007–1023.
(51) Sadlej, A. J. *Collect. Czech. Chem. Commun.* **1988**, *53*, 1995–2016.
(52) ACES II program is a product of the Quantum Theory Project, University of Florida. Authors: Stanton, J. F.; Gauss, J.; Watts, J. D.; Nooijen, M.; Oliphant, N.; Perera, S. A.; Szalay, P. G.; Lauderdale, W. J.; Kucharski, S. A.; Gwaltney, S. R.; Beck, S.; A. Balková, Musiał, M.; Bernholdt, D. E.; Baeck, K. -K.; Sekino, H.; Rozyczko, P.; Huber, C.; Bartlett, R. J. Integral packages included are VMOL (Almlöf, J.; Taylor, P.), VPROPS (Taylor, P. R.), and a modified version of the ABACUS integral derivative package (Helgaker, T. U.; Jensen, H. J. Aa.; Olsen, J.; Jorgensen, P.; Taylor, P. R.).
(53) Moore, C. E. Atomic Energy Levels. Natl. Bur. Stand. (U.S.), Circ.1949, Vol. *467*.